

Direct Summation of the Madelung Constant using Axial Multipoles

Joven V. Calara ^{*1} and Jan D. Miller²

¹Dept of Engineering, Salt Lake Community College

²Dept of Metallurgy, University of Utah

March 18, 2025

Abstract

A direct summation method for the Madelung constant calculation is presented where a crystal lattice is constructed from linear arrays of charges or axial multipoles. An array is designed to have vanishing low order electric moments such that its potential at the origin from a distance r decays at least as fast as r^{-5} , but preferably as fast as r^{-13} . High potential decay rates render the summation absolutely convergent in up to 6 dimensions. Convergence speed increases with higher decay rates. It is also shown that the limit approached by the summation is independent of the growth geometry. Madelung constants for NaCl bulk, surface, and edge lattice points are calculated, as well as on off-lattice points such as interstitial positions and external neighborhoods of surfaces. Bulk CsCl Madelung constant is also calculated. Up to 3 dimensions, accuracy of 13 decimal places are attained within 40 nearest neighbor distance from the reference ion.

Introduction

Electrostatic or Coulombic forces account for a large share of the binding energies in ionic crystals, and therefore strongly influence their properties. But the long range properties of Coulombic forces make the seemingly straightforward calculation of total electrostatic potentials quite deceptive.

In the interior of the lattice, the electrostatic potential energy of an ion is the sum of the potentials due to all the other ions in the crystal. For an infinite NaCl lattice as example, the potential energy U of an ion at the origin of a coordinate system parallel to the Bravais vectors is the sum of all contributions from the other ions;

$$U = \frac{e^2}{4\pi\epsilon_0\alpha} \sum'_{ijk} \frac{(-1)^{i+j+k}}{\sqrt{i^2 + j^2 + k^2}} \quad (1)$$

where i,j,k are the integer coordinates of the alternating Na and Cl ions, e is the electronic charge, ϵ_0 is the permittivity of vacuum, and α a characteristic lattice parameter, often the nearest neighbor distance. The prime on the summation sign indicates self potential of the ion on the origin is excluded.

The summation factor is identified as the Madelung constant. Following conventional practice for brevity, the pre-sum factor $e^2/4\pi\epsilon_0\alpha$ will be dropped but is implied in expressions for potentials in the following discussions.

The sum is conditionally convergent (i.e. it will diverge to $\pm\infty$ if all charges are of one sign). As such, it may converge to different limits, or not at all, depending on the order the terms are summed. The two general methods of attacking the convergence problems are direct summations and integral methods. Direct summation is the literal application of equation (1), where potentials from individual or grouped charges are added as they are encountered by expanding volumes. A widely known direct summation is that of Evjen[3],

*jcalara@slcc.edu, jvcalara@yahoo.com, jan.miller@utah.edu

who grouped the NaCl charges into neutral shells of increasing size around a reference ion, thereby speeding up the convergence. Of the integral methods, Ewald's[4] approach is the most widely known and involves integration in reciprocal space. This paper focuses only on a direct summation.

The attraction of the direct summation is its apparent, but deceiving, simplicity. Evjen's method was a model advancement, but is dependent on identifying neutral shells around a reference ion, which is not always easy or possible. A natural approach is to add ions as they are encountered by expanding spherical shells[6][11]. The shells were found to be non-neutral and resulted in seemingly random swings above and below the target value. Other attempts use the expanding neutral, prismatic shells dictated by the lattice's Bravais vectors[8]. This works well with NaCl and CsCl, but not easily applicable to the complex structures such as the perovskite and rutile lattices.

Elimination of low order electrical moments has been recognized as a path to improving convergence speeds[12], though Gelle[5] indicated how difficult it can be for unit cells. The present paper describes how the use of axial multipoles greatly facilitates cancellation of low order electrical moments and thus leads to successful calculation of Madelung constants by direct summation.

Axial Multipoles

Axial multipoles, as defined here, are sets of charges that lie on a single axis. When properly designed, they can be assembled to reproduce a target lattice. Their use in obtaining Madelung constants was first proposed by the authors[7]. That concept is developed here in detail and placed on a clearer mathematical basis. The central idea was to design an axial multipole such that its potential, measured at the origin, falls off, or decays, rapidly with its distance from it. Fast decay rates are shown to give excellent convergence properties to the array.

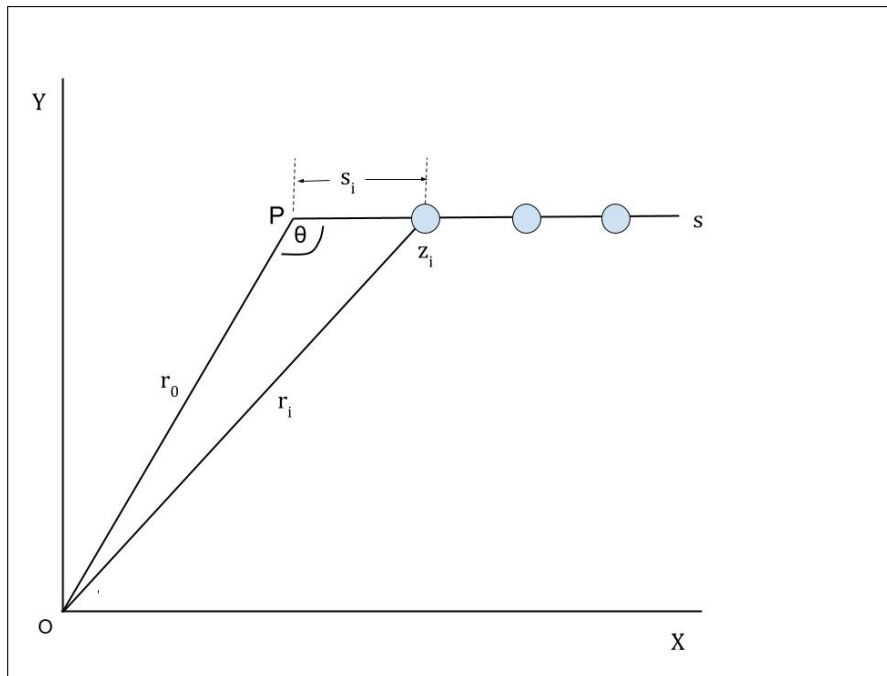


Figure 1: Charge array

Consider a linear array of point charges (Figure 1), $z_i, i = 1, n$, along an arbitrary line S parallel to the x-axis. Point P on S is in the near neighborhood of the array but is otherwise arbitrarily located, and is at a distance

r_0 from the point O, the XY coordinate origin. Line OP makes an angle θ with line S. Charge z_i is at a distance s_i from P and at distance r_i from the origin O.

The potential ϵ_i at the origin due to charge z_i is;

$$\epsilon_i = \frac{z_i}{r_i} = \frac{z_i}{\sqrt{r_0^2 + s_i^2 - 2r_0s_i\cos\theta}} = \frac{z_i}{r_0} \left(1 + \left(\frac{s_i}{r_0}\right)^2 - 2\frac{s_i}{r_0}\cos\theta \right)^{-\frac{1}{2}} \quad (2)$$

Expanding the radical into a Taylor series and collecting like powers of (s_i/r_0) ;

$$\epsilon_i = \frac{z_i}{r_0} \left(P_0 + \frac{s_i}{r_0} P_1 + \left(\frac{s_i}{r_0}\right)^2 P_2 + \left(\frac{s_i}{r_0}\right)^3 P_3 + \left(\frac{s_i}{r_0}\right)^4 P_4 \dots \right) \quad (3)$$

where P_i s are the Legendre polynomials (in $\cos\theta$), the first few of which are;

$$P_0 = 1 \quad P_1 = \cos\theta \quad P_2 = \frac{1}{2}(3\cos^2\theta - 1) \quad P_3 = \frac{1}{2}(5\cos^3\theta - 3\cos\theta)$$

The total potential ϵ_T from charge array of n members is then

$$\epsilon_T = \sum_{i=1}^n \epsilon_i = \frac{P_0}{r_0} \sum_{i=1}^n z_i + \frac{P_1}{r_0^2} \sum_{i=1}^n z_i s_i + \frac{P_2}{r_0^3} \sum_{i=1}^n z_i s_i^2 + \frac{P_3}{r_0^4} \sum_{i=1}^n z_i s_i^3 + \frac{P_4}{r_0^5} \sum_{i=1}^n z_i s_i^4 \dots \quad (4)$$

If the array is far from origin, with $s_i \ll r_0$, any term in the series would be much larger than the next, and ϵ_T becomes essentially equal to the first non-zero, or leading, term.

From electrostatics, the quantity

$$\frac{P_k}{r_0^{k+1}} \sum_{i=1}^n z_i s_i^k$$

is identified as monopole potential for $k = 0$, then dipole, quadrupole, octopole, and hexadecapole potentials of orders $k = 1, 2, 3, 4$ respectively. Higher orders will simply be called as k^{th} -order poles.

High-order axial multipoles

2⁴-pole RU-5 (Hexadecapole)

Of particular interest in equation (4) is that a potential term decays at a faster rate with distance r_0 the farther down it is in the sequence. So if, for example, we wish the collective potential of the array to decay at a rate proportional to r_0^{-5} , then each of the first 4 terms on the right side of equation (4) must vanish identically. This gives us four simultaneous equations (after canceling out the pre-sum factors);

$$\sum_{i=1}^n z_i = 0; \quad \sum_{i=1}^n z_i s_i = 0; \quad \sum_{i=1}^n z_i s_i^2 = 0; \quad \sum_{i=1}^n z_i s_i^3 = 0 \quad (5)$$

If further $s_i \ll r_0$, terms after the first remaining in equation 4 can be neglected, giving;

$$\epsilon_T = \frac{P_4}{r_0^5} \sum_{i=1}^n z_i s_i^4 \quad (6)$$

which has the desired potential decay rate.

Equation (5)'s 4 sub-equations require that $n > 4$ to avoid the trivial solution $z_i = 0$ ($i = 1, 2, 3, 4$). We select $n = 5$ to minimize calculations, which in turn requires a fifth equation for a unique, non-trivial solution.

The form that the fifth equation takes can be illustrated by taking the prototypical one dimensional alternating charge NaCl lattice as an example. Without loss of generality we coincide line S in Figure (1) with the x-axis, and lay down the five charges z_i in the sequence (+ - + - +) on positions $x_i = i, i = 1, 2, 3, 4, 5$. Equations (5) become;

$$\sum_{i=1}^5 z_i = 0; \quad \sum_{i=1}^5 z_i x_i = 0; \quad \sum_{i=1}^5 z_i x_i^2 = 0; \quad \sum_{i=1}^5 z_i x_i^3 = 0 \quad (7)$$

The fifth equation can now be used to specify that the sum of the positive charges equals unity, a condition necessary for the replication of the NaCl lattice's unitary charges when the arrays are assembled, viz;

$$z_1 + z_3 + z_5 = 1 \quad (8)$$

Casting the combined set of equations (7) and (8) in matrix form, we get;

$$\begin{bmatrix} 1 & 1 & 1 & 1 & 1 \\ 1 & 2 & 3 & 4 & 5 \\ 1 & 2^2 & 3^2 & 4^2 & 5^2 \\ 1 & 2^3 & 3^3 & 4^3 & 5^3 \\ 1 & 0 & 1 & 0 & 1 \end{bmatrix} \begin{bmatrix} z_1 \\ z_2 \\ z_3 \\ z_4 \\ z_5 \end{bmatrix} = \begin{bmatrix} 0 \\ 0 \\ 0 \\ 0 \\ 1 \end{bmatrix} \quad (9)$$

Equation (9) can be solved with any computer algebra system to give the 5-member axial multipole (Figure 2), which is a 2^4 -pole or *hexadecapole*.

For reasons that will be apparent, we shall refer to this array as **RU-5** (“**5**-membered **R**epeating **U**nit”) for NaCl;

$$[z_1 \quad z_2 \quad z_3 \quad z_4 \quad z_5] = \left[\frac{1}{8} \quad -\frac{1}{2} \quad \frac{3}{4} \quad -\frac{1}{2} \quad \frac{1}{8} \right]$$

Figure 2: 5-membered array (RU-5), a hexadecapole.

2^{12} -pole, RU-13

The rules by which RU-5 is designed apply as well to higher order poles. Skipping the next few higher poles, a 2^{12} -pole **RU-13** is derived in the Appendix. In brief, we aim to build an array whose potential decays at a rate proportional to r_0^{-13} . The first 12 terms of equation (4) are each set to vanish identically, yielding 12 equations. Likewise, the 13th equation is then used to set the sum of positive charges equal to unity.

The resulting 13 member RU-13's is shown in abbreviated form in Figure 3 and in full in Figure 9 of the Appendix. The common multiplier $1/2048$ is factored out for clarity;

$$\begin{bmatrix} z_1 & z_2 & z_3 & z_4 & \dots & \dots & z_{10} & z_{11} & z_{12} & z_{13} \end{bmatrix} = \frac{1}{2048} * [(1 \quad -12 \quad 66 \quad -220 \quad \dots \quad \dots \quad -220 \quad 66 \quad -12 \quad 1)]$$

Figure 3: 13-membered array (RU-13) (see Appendix for full expression).

Distance Test

Equations (6) and (16 in Appendix) state that RU-5 and RU-13 potentials fall off proportional to r_0^{-5} and r_0^{-13} respectively. This can be verified by placing them at different distances from the origin, e.g.

centered at $x = 15$ and $x = 30$. With a distance ratio of 2, the ratio of potentials from those locations should be approximately 2^5 for RU-5 and 2^{13} for RU-13.

We obtain for RU-5;

$$\frac{\text{potential}(x = 15)}{\text{potential}(x = 30)} = \frac{4.04 \times 10^{-6}}{1.24 \times 10^{-7}} = 32.54 = 2^{5.02} \quad (10)$$

We obtain for RU-13;

$$\frac{\text{potential}(x = 15)}{\text{potential}(x = 30)} = \frac{1.85 \times 10^{-10}}{1.32 \times 10^{-14}} = 13,913 = 2^{13.7} \quad (11)$$

Thus confirming the decay rates given by the equations.

A decay rate of r_0^{-5} is enough to overcome the r_0^3 growth in numbers of summation units in 3D lattices to guarantee convergence.

The distance test should be valid in determining the potential order of a given point charge array of any geometry, without reference to, or knowledge of, its electric moments, and allow estimation of its convergence properties.

Construction of the NaCl Lattice

Taking the array RU-5 as an example, to construct a neutral line of NaCl we place copies of RU-5 on successive positions that match charge signs. Referring to Figure (4), several RU-5 units are aligned in such like manner, and when are placed down on the x-axis, the unitary charges of Na and Cl are reproduced.

The terminals ends always consist of the same set of fractional charges while the interior segment of unit charges lengthens.

It is easy to verify that RU-13 will also replicate the linear NaCl lattice, albeit with a different set of fractional charges at the terminal ends (see figure (10) in Appendix).

Figure 5 shows how a plane of NaCl in turn, is formed from lattice lines described above. The plane could stand alone as a single planar lattice, or as part of a 3D NaCl crystal.

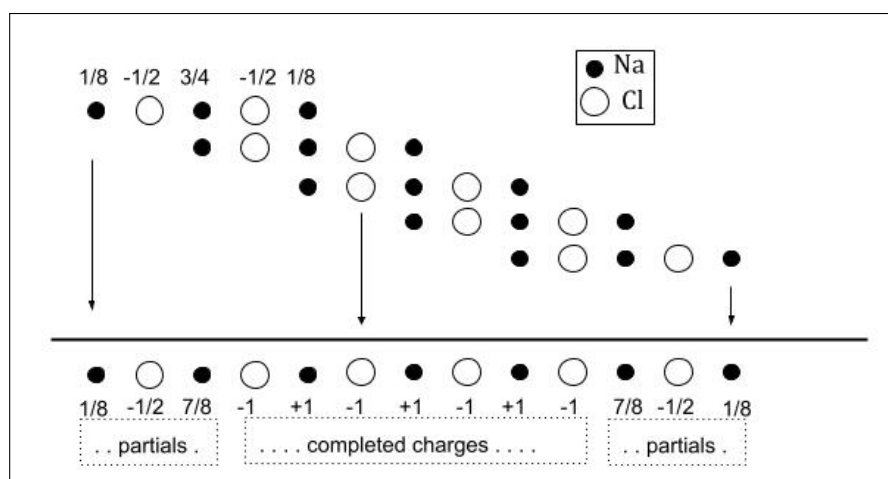


Figure 4: NaCl lattice being assembled from RU-5.

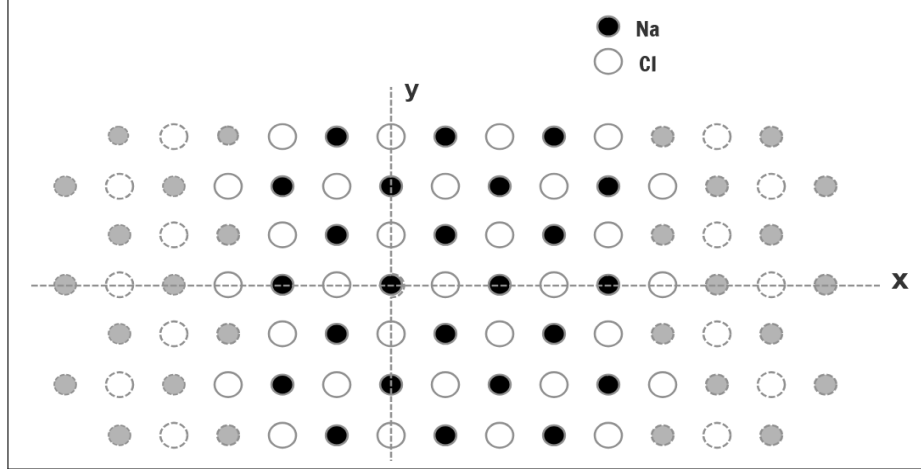


Figure 5: NaCl plane with whole (solid circles) and partial (dashed circles) charges during construction with RUs. The RUs are aligned parallel to the x-axis.

Madelung Constants

Madelung constant 1D NaCl

Consider a one-dimensional (1D) NaCl infinite $(-\infty, +\infty)$ lattice with alternating Na, Cl located on integer x , with Na at the origin. The potential ϵ_{1D} , at the origin i.e, the Madelung constant, is the sum of potentials from all the other charges, viz;

$$\epsilon_{1D} = 2(1 - 1/2 + 1/3 - 1/4 + 1/5 - 1/6 \dots) \quad (12)$$

The factor 2 takes advantage of the 2-fold symmetry of the lattice. Inside the parentheses in Equation (12) is the familiar alternating harmonic series, which is conditionally convergent and has the closed form solution $\ln(2)$, so;

$$\epsilon_{1D} = 2 \ln(2) = 1.3862 \ 9436 \ 1119 \ 8906 \ 1883 \dots \quad (13)$$

The partial sum of the alternating harmonic series to the n^{th} term is in error approximately equal to $(n+1)^{th}$ term, the first one omitted. Thus the error after 100 terms is about ± 0.01 , and an accuracy of 4 decimal places will require about 10,000 terms - a very slow converging series indeed.

The convergence speeds of the alternating harmonic series and those of the RU-5 and RU-13 axial multipole constructions will be compared side by side.

The RUs are centered on successive Na sites starting at the origin and proceeding symmetrically outwards, and the potentials accumulated at the same time. Any RU member falling on the origin is excluded from the sum.

The results of the three methods are presented in Table 1, where n is the nearest neighbor count along the positive x -axis. Note the very fast convergence of RU-13.

Planar (2D) NaCl, Center and Edge Madelung Constants

In the next examples we will use the RU-13 unit exclusively because of its fast convergence properties.

Table 1: NaCl $2\log(2)$ approximations, comparing convergence of the alternating harmonic series, RU-5, and RU-13 at increasing n -multiples of nearest neighbor distance from reference ion. Underlined last digits mark departure from correct value. Accuracy to 14 decimal places is attained with RU-13 at a very short distance.

Length n	Method		
	Alt-Harmonic	RU-5	RU-13
4	1. <u>6</u>	1.38 <u>7</u>	1.38 <u>3</u>
10	1. <u>5</u>	1.386 <u>3</u>	1.386294 <u>37</u>
20	1.3 <u>7</u>	1.38629 <u>8</u>	1.3862943611 <u>2</u>
40	1.3 <u>5</u>	1.386294 <u>6</u>	1.38629436111989
100	1.3 <u>7</u>	1.38629436 <u>8</u>	
1000	1.38 <u>5</u>	1.3862943611 <u>2</u>	

Although RU-13 has more members than e.g RU-5 for calculation, faster convergence of RU-13 more than compensates by needing much fewer RUs.

In all NaCl lattice constructions, the RUs, oriented parallel to the x-axis, are centered on Na sites (the center of RU-13 is an Na by choice) beginning with the reference Na at the origin and proceeding outwards in any uniform growth geometry. For emplacing RUs, Na sites are located at coordinates (i, j) if $\text{mod}((i + j), 2) = 0$. The potentials are calculated and accumulated, but any charge falling on the origin is excluded from the sum.

For the edge-of-plane potential we simply exclude, e.g., the positive y-axis. The results are shown in Table 2.

At $n = 30$, the planar center Madelung constant (MC) agrees with Burrows[2] to all places shown. There are no corresponding values found for the planar edge. However, a brief consideration would show that one-half of the planar center MC plus one-half MC of the 1D lattice from Table 1 should equal the planar edge MC, to wit;

$$\text{Edge MC} = (1/2) \times (1.615542626713 + 1.386294361119) = 1.500918493916$$

which agrees with the direct sum in Table 2.

Table 2: Planar NaCl center and edge sums at n -multiples of nearest neighbor distance from reference ion. Underlined digits mark departure from Burrows's.

Length n	Planar Madelung constant	
	Center	Edge
10	1.615542 <u>4</u>	1.500918518
20	1.6155426267 <u>2</u>	1.500918493925
30	1.615542626713	1.500918493916
<i>Burrows</i> [2]	1.615542626713	(None in literature)

**3D NaCl, Bulk, Surface, and Edge Madelung Constants.
Growth Geometry**

Growth Geometry Effects

In the case of 3D summation, a natural growth geometry, more intuitive from a coding standpoint, is generated by a nested indexing on x, y and z coordinates aligned with the Bravais vectors, thus defining a cubical growth. The other natural choice is spherical growth where ions encountered at each growth step are added to the sum. The two geometries are compared side by side in Table 3.

The speed of convergence in terms of crystallite size is seen to be the same in either geometry, and the same limits are attained. The absence of growth shape effect is not surprising. The rapid decay of potential of RU-13 implies that regions that are sufficiently distant will have essentially zero potential contributions, and therefore it is immaterial what their shapes are. That the 40th shell was sufficiently distant was an unexpected, but welcome, surprise.

It should be mentioned that calculations with RU-13 approach the limit of accuracy for double precision arithmetic, and so accuracy beyond 14 decimal places is not be expected.

Table 3: 3D NaCl Madelung constants with RU-13, **cubical** vs **spherical** growth, with increasing n-multiples of nearest neighbor distance along the x-axis. Accuracy to 13 decimal places were attained in both cases within $n = 40$. Underlined (last) digits mark departure from accepted value.

Shells n	Growth Geometry	
	Cubic	Spherical
3	1. <u>6</u>	1. <u>5</u>
7	1.747564 <u>9</u>	1.7475 <u>3</u>
10	1.74756459 <u>7</u>	1.7475645 <u>3</u>
20	1.74756459463 <u>6</u>	1.7475645946 <u>6</u>
30	1.747564594633 <u>2</u>	1.747564594633 <u>6</u>
40	1.7475645946331 <u>7</u>	1.74756459463318
<i>OEIS</i> [9]	1.7475645946331821	

Surface and Edge Madelung constant

Table 4 shows the direct sums for the 3D NaCl surface and edge MCs. Surface MC was obtained by excluding the negative segment of either y or z axis, and the edge MC by excluding both of them. The RU-13 us aligned along the x-axis, so the x-axis is not used in the exclusion process because that will involve truncation of the RUs, which results in low order multipole fragments on the surface, which in turn slows down convergence. Included also in the table are Madelung constants derived from easily established formulas. If we define

- $M1 = 1.386294361119890$; 1D NaCl (line) MC ($2\ln(2)$)
- $M2 = 1.615542626713$; 2D NaCl (planar) MC
- $M3 = 1.74756459463318$; 3D NaCl (bulk) MC
- $M_{surf} =$ surface MC of 3D NaCl
- $M_{edge} =$ edge MC of 3D NaCl

then

$$\begin{aligned}
 M_{surf} &= \frac{1}{2}(M3 + M2) \\
 M_{edge} &= \frac{1}{4}M3 + \frac{1}{2}(M2 + M1)
 \end{aligned}
 \tag{14}$$

These agree to all 12 digits with Baker’s[1] cited “true” values.

Table 4: 3D NaCl Surface and Edge MCs. Size of lattice is 40 nearest neighbors from origin along the x-axis.

Method	3D MCs	
	Surface	Edge
Direct sum	1.6815536106730	1.5912360522947
Formulas	1.6815536106730	1.5912360522947
<i>Baker</i> [1]	1.68155361067	1.59123605229

4D, 5D, and 6D Hyperdimensional NaCl

Programmatically, going from 3D to higher dimensions involves simply adding the requisite levels to the nested iteration on coordinates, e.g., iterating on [x y z] of 3D-cube to [x y z w] of 4D-hypercube, and so on. Locating an Na site for laying RU-13 remains the same; $mod(x + y + z + w + ..), 2) = 0$, and the RU-13s are still oriented parallel to the x-axis.

Table 5 lists some results. Agreement with available literature values is good, but noticeably degrades at higher dimensions.

The number of RUs (and therefore computations time) increases exponentially with n^N , where n

Table 5: Madelung constants for hypercubic NaCl of 4, 5, and 6 dimensions. Summation distance is 30 shells. For the same crystallite size along one axis, accuracy decreases with higher dimensionality.

Shells=30 Source	Dimensionality		
	4D	5D	6D
This work	1.839399084036	1.9093378158	1.96555704
<i>Burrows</i> [2]	1.83939908404504	1.90933781561876	1.96555703900907

is the number of nearest neighbors along the positive x-axis, and N the dimension chosen. So if $n = 30$, then going from $N = 3$ to $N = 4$ increases computation times by $30^4/30^3 = 30$ times, 900 times going to $N = 5$, and 27,000 times going to $N = 6$. These can be reduced an order of magnitude by identification of reflection and rotation symmetries to count multiple copies of an RU with the same potential to avoid recalculating them. For example, for the 6D case, calculation time was reduced from 15 hours to 1/2 hour by symmetry considerations. Still, higher accuracies at higher dimensions proved daunting on a desktop computer (Dell 7050 i7 Optiplex).

Potential plots on exterior and interior planes of NaCl

Potentials at arbitrary off-lattice sites are just as easily obtained as for lattice ion sites. Figure (6) illustrates maps of potentials on a plane located parallel to a (001) cleavage plane of NaCl at different elevations. Contours projected on the X-Y plane indicate relative positions of Na, Cl on the cleavage plane, coinciding vertically with

peaks and valleys of the potential surface. The z-axis represents the MC of a unit positive test charge at each point on the surface plot. The peak-to-peak amplitude diminished 90% going from 1-unit elevation to 1.5 units.

Similar maps can be made for the interior lattice spaces with equal facility, as shown on Figure (7).

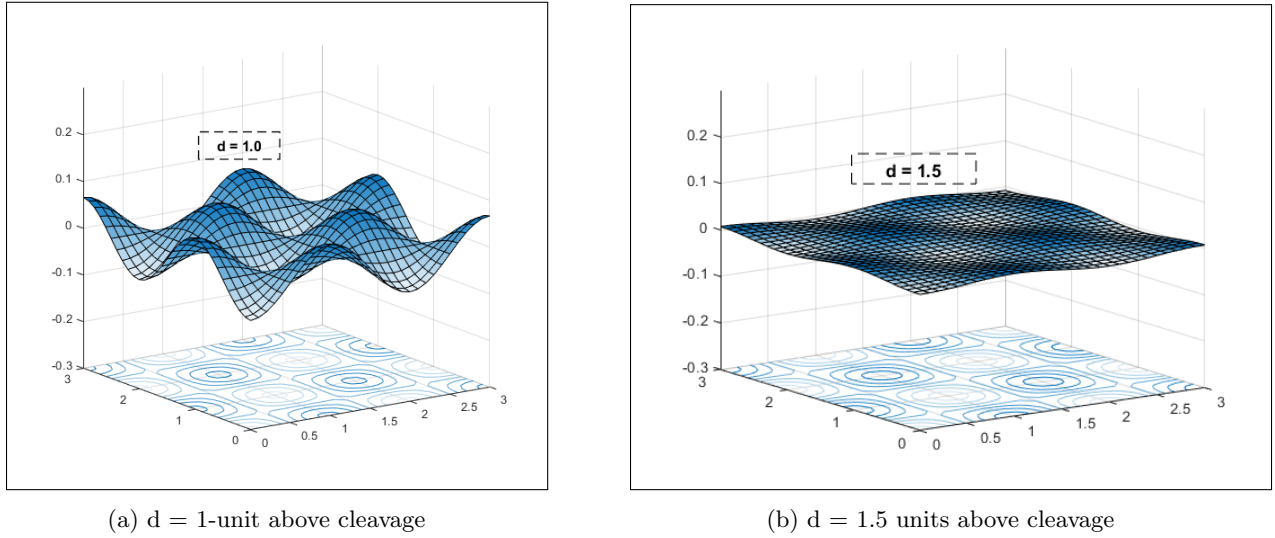


Figure 6: "Madelung constants" on a 3×3 unit cells square off-lattice plane at different heights d above an NaCl (001) cleavage plane. One unit is Na-Cl spacing. Note how potential plot flattens to near zero at $d = 1.5$, losing 90% of its amplitude from $d = 1$.

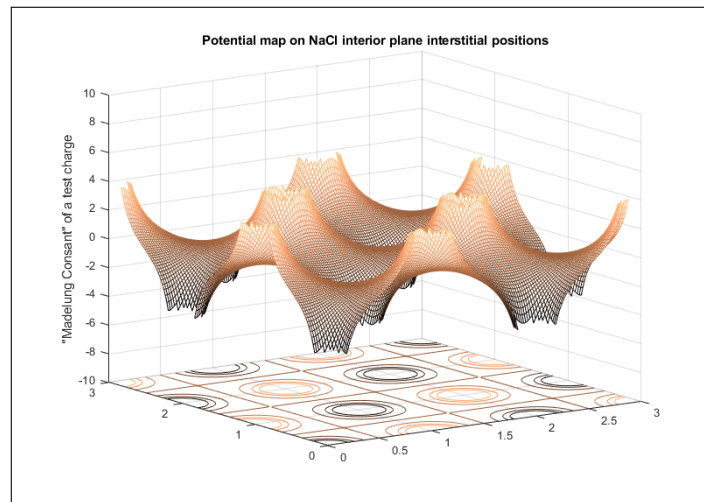


Figure 7: Potential plot ("Madelung constant") on an interior (001) NaCl plane interstitial positions. Potential goes to $\pm\infty$ at lattice ion sites.

CsCl 3D Madelung Constant

The CsCl lattice's unit cell may be viewed as a cube 2-units wide with Cl at the corners and Cs at the body center, as depicted in Figure (8).

The line of charges along the body diagonal consists of alternating, equispaced Cs and Cl ions. The CsCl lattice can thus be also constructed from an RU-13 axial multipole, with $\sqrt{3}$ charge spacing and oriented along the diagonal. To build the lattice the RU-13s are centered on each Cs site at coordinates (i, j, k) that satisfy $\text{mod}(i + j + k, 2) = 0$. Summation results are shown in Table (6).

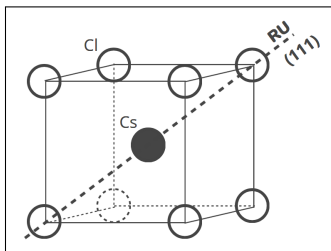


Figure 8: CsCl unit cell, RU-13 orientation.

Table 6: 3D CsCl Madelung constant with **RU-13** axial multipole, referred to Cs-Cl nearest neighbor spacing, on diagonal. Accuracy to 13 decimal places were attained within $n = 30$. Underlined (last) digits mark departure from accepted value.

Shells	
n	Madelung constant
5	1.7629
10	1.762674772
20	1.7626747730708
30	1.76267477307094
<i>OEIS</i> [10]	1.7626747730709883

Conclusions

The method of repeating unit with axial multipoles was successful in reproducing Madelung constants with fast convergence to high accuracies. Madelung constants of NaCl lattices of 1 to 6 dimensions were calculated. Using the axial multipole R-13, 13 decimal places bulk NaCl Madelung constant was obtained in less than 1 second on a desktop computer. For higher dimensional hypercubes, calculations slowed down as expected. Potential maps above the (100) cleavage surface of NaCl, as well as on an interior ion plane were constructed.

The method has its limitations. It requires the presence of neutral and absolutely colinear arrays of lattice ions. Therefore, nitrates, carbonates and similar complex anions with off-axis charge centers cannot be treated by the method as it currently stands. Polar cleavages, such as the (110) plane of NaCl, are not susceptible to the method, as it would entail truncation of the axial multipole near the surface, leaving behind a residue with a net charge that could lead to either a very slow convergence or even divergence.

Axial multipoles beyond R-13 are possible, but will require the rare 128-bit hardware-based quadruple precision arithmetic to maintain speed. Software based high precision arithmetic is readily available, but has been known to be orders of magnitude slower than the hardware based ones.

Future research will examine axial multipoles with two different charge spacings (CaF_2), multispaced as well as asymmetrical (ZnS sphalerite), and intersecting (CaTiO_3 perovskite). The latter also requires two different axial multipoles.

Appendix

Construction of 13-membered NaCl RU-13 axial multipole

We look again at equation (4);

$$\epsilon_T = \frac{P_0}{r_0} \sum_{i=1}^n z_i + \frac{P_1}{r_0^2} \sum_{i=1}^n z_i s_i + \frac{P_2}{r_0^3} \sum_{i=1}^n z_i s_i^2 + \frac{P_3}{r_0^4} \sum_{i=1}^n z_i s_i^3 + \frac{P_4}{r_0^5} \sum_{i=1}^n z_i s_i^4 \dots \quad (\text{Eqn 4 revisited})$$

If we want an NaCl RU's potential to decay proportional to r_0^{-13} , then all terms with the factor r_0^{-k} , $k = 1, 2, 3, \dots, 12$ must each be equal to zero. If we set $s_i = i$ such as it would if we lay the RU charges on integer x beginning at $x=1$, this gives 12 equations, after cancelling out the pre-sum factors;

$$\sum_{i=1}^n z_i i^{k-1} = 0 \quad k = 1, 2, 3, \dots, 11, 12 \quad (15)$$

If $s_i \ll r_0$, equation 4 then reduces to;

$$\epsilon_T = \frac{P_{12}}{r_0^{13}} \sum_{i=1}^n z_i s_i^{12} \quad (16)$$

which has the desired potential decay rate.

The 12 equations need to be augmented with a 13th equation or more for a non-trivial solution ($z_i = 0; i = 1, 2, 3, \dots, 12$). That in turn requires the RU to have at least 13 members. We will use $n = 13$ for this derivation for economy of computation.

The 13th equation will be used, as before, to set the positive charges sum to unity. For consistency we will select the central charge, the z_7 , to be positive, so;

$$z_1 + z_3 + z_5 + z_7 + z_9 + z_{11} + z_{13} = 1 \quad (17)$$

With $n = 13$, combining equations (15) and (17) into a 13×13 matrix yields;

$$\begin{bmatrix} 1 & 1 & 1 & 1 & 1 & 1 & 1 & 1 & 1 & 1 & 1 & 1 & 1 \\ 1 & 2 & 3 & 4 & 5 & 6 & 7 & 8 & 9 & 10 & 11 & 12 & 13 \\ 1 & 2^2 & 3^2 & 4^2 & 5^2 & 6^2 & 7^2 & 8^2 & 9^2 & 10^2 & 11^2 & 12^2 & 13^2 \\ 1 & 2^3 & 3^3 & 4^3 & 5^3 & 6^3 & 7^3 & 8^3 & 9^3 & 10^3 & 11^3 & 12^3 & 13^3 \\ \vdots & \vdots & \vdots & \vdots & \vdots & \vdots & \vdots & \vdots & \vdots & \vdots & \vdots & \vdots & \vdots \\ 1 & 2^{10} & 3^{10} & 4^{10} & 5^{10} & 6^{10} & 7^{10} & 8^{10} & 9^{10} & 10^{10} & 11^{10} & 12^{10} & 13^{10} \\ 1 & 2^{11} & 3^{11} & 4^{11} & 5^{11} & 6^{11} & 7^{11} & 8^{11} & 9^{11} & 10^{11} & 11^{11} & 12^{11} & 13^{11} \\ 1 & 0 & 1 & 0 & 1 & 0 & 1 & 0 & 1 & 0 & 1 & 0 & 1 \end{bmatrix} \begin{bmatrix} z_1 \\ z_2 \\ z_3 \\ z_4 \\ \vdots \\ z_{11} \\ z_{12} \\ z_{13} \end{bmatrix} = \begin{bmatrix} 0 \\ 0 \\ 0 \\ 0 \\ \vdots \\ 0 \\ 0 \\ 1 \end{bmatrix} \quad (18)$$

Solving, we get the 13 charges of RU-13;

$$\frac{1}{2048} * [1 \quad -12 \quad 66 \quad -220 \quad 495 \quad -792 \quad 924 \quad -792 \quad 495 \quad -220 \quad 66 \quad -12 \quad 1]$$

Figure 9: RU-13 members, with 1/2048 factored out

Stacking RU-13 on the x-axis on successive locations will reconstruct the 1D NaCl lattice, terminated by partial charge assemblies. Shown below is the right end termination plus a few completed unit charges at some stage of construction.

$$\left[-1 \quad 1 \quad -1 \quad \frac{2047}{2048} \quad \frac{-2036}{2048} \quad \frac{1981}{2048} \quad \frac{-1816}{2048} \quad \frac{1486}{2048} \quad \frac{-1024}{2048} \quad \frac{562}{2048} \quad \frac{-232}{2048} \quad \frac{67}{2048} \quad \frac{-12}{2048} \quad \frac{1}{2048} \right]$$

Figure 10: Terminus detail of 1D NaCl lattice from RU-13.

References

- [1] A.D. Baker and M.D. Hanusa Cooper. “Corner ion, edge-center ion, and face-center ion Madelung expressions for sodium chloride”. In: *J. Math. Chem.* 49 (2011), pp. 1192–1198.
- [2] R. Burrows and S. Cooper. “The Madelung constant in N dimensions”. In: *Proc. Royal Soc. A* 478 (2022).
- [3] H.M. Evjen. In: *Phys. Rev* 39 (1932), p. 675.
- [4] P.P. Ewald. In: *Ann. Phys.* 64 (1921), p. 253.
- [5] A. Gelle. “Fast calculation of the electrostatic potential in ionic crystals by direct summation method”. In: (2007). URL: <https://arxiv.org/abs/0711.2888>.
- [6] W.A. Harrison. In: *Phys. Rev.B* 73 (2006), p. 212103.
- [7] J.D. Miller and J.V. Calara. “Determination of Madelung Constants for infinite and semi-infinite lattices by direct summation”. In: *J. Chem. Phys.* 65.2 (1976), pp. 843–844.
- [8] R.D. Murphy. In: *Indian J. Chem* 35A (1996), pp. 1102–1103.
- [9] OEIS Foundation Inc. 2024. URL: <https://oeis.org/A085469>.
- [10] OEIS Foundation Inc. 2024. URL: <https://oeis.org/A181152>.
- [11] R.M. Pratt. “Madelung Constants for Ionic Crystals using the Ewald Sum”. In: *Jurnal Kejuruteraan* 13 (2001), pp. 21–39.
- [12] Dieter Wolf. “Simulation of Ionic Surfaces from an Absolutely Convergent Solution of the Madelung Problem”. In: *Springer Proceedings in Physics* 80 (1995), p. 57.